

Boltzmann-Gibbs states in topological quantum walks: Fidelity analysis of Phase Transitions

Bruno Mera^{1,2,3}, Chrysoula Vlachou^{4,5}, Nikola Paunković^{4,5} and Vítor R. Vieira^{1,2}

¹ *CeFEMA, Instituto Superior Técnico, Universidade de Lisboa, Av. Rovisco Pais, 1049-001 Lisboa, Portugal*

² *Departamento de Física, Instituto Superior Técnico, Universidade de Lisboa, Av. Rovisco Pais, 1049-001 Lisboa, Portugal*

³ *Physics of Information and Quantum Technologies Group, Instituto de Telecomunicações, 1049-001 Lisbon, Portugal*

⁴ *SQIG-Security and Quantum Information Group, Instituto de Telecomunicações, 1049-001 Lisbon, Portugal and*

⁵ *Departamento de Matemática, Instituto Superior Técnico, Universidade de Lisboa, Av. Rovisco Pais, 1049-001 Lisboa, Portugal*

We perform the fidelity analysis for Boltzmann-Gibbs-like states in order to investigate whether the topological order of one-dimensional fermionic systems at zero temperature is maintained at finite temperatures. We use quantum walk protocols that are known to simulate topological phases and the respective quantum phase transitions for chiral symmetric Hamiltonians. We show, by means of the fidelity analysis and the behaviour of edge states, that no thermal-like phase transitions occur as temperature increases, i. e., the topological behaviour is washed out gradually.

PACS numbers: 05.30.Rt, 05.30.-d, 03.67.-a, 03.65.Vf

I. INTRODUCTION

Since the seminal paper of Haldane [8], where the anomalous Hall insulator in the honeycomb lattice was first discovered, there has been an intense investigation on the subject of topological phases of matter. To characterize topological phases, topological invariants such as Chern numbers [22] and the Berry geometric phases [5], as well as non-local string parameters [30], have been used as standard signatures of topological orders. For a review of the subject, see for example [3]. In this context of zero-temperature quantum phase transitions, the critical behaviour of systems featuring topological order is accompanied by the existence of the so-called edge states at the boundary between two distinct topological phases [27], [20]. Moving to open quantum systems, whose states of matter are given by mixed, rather than pure, states, it is natural to ask if the topological order is still present, and investigate which are the appropriate quantities (“topological order parameters”) to describe the possible phase transitions. Various types of the mixed-state generalizations of geometric phases [23], as well as the Chern values [19], were used to infer topological phase transitions of open systems (thermal and/or non-equilibrium). In particular, it was shown that the non-trivial Uhlmann phase, the generalization of the pure-state Berry phase, vanishes above certain “critical” temperature T_U , for the case of the one- and two-dimensional fermionic systems given by quadratic Hamiltonians [26], [25]. Nevertheless, the relevance of the particular Uhlmann phase to the observable properties that reflect topological orders of the systems considered, stays as an interesting open question, see for example [2].

In addition to the standard local symmetry-breaking and the above mentioned global topological order parameters, several information-theoretic quantities were used to study phase transitions, such as various entanglement measures [7, 9, 10] and the fidelity [1, 16, 17, 29, 31]. Being the measure of the distinguishability between two quantum states, the fidelity was argued to capture all the possible orders, and was used in numerous studies of both zero- and finite-temperature symmetry-breaking phase transitions, as well as of Kosterlitz–Thouless transitions and topological orders [6], [15]. In [28] the authors analyzed the intimate connection between the pure-state fidelity and the Berry phase, showing that the fidelity-induced Riemannian metric and the Berry connection are the real and the imaginary part, respectively, of the so-called quantum geometric tensor. In the context of mixed thermal states, the fidelity and the Uhlmann phase were studied for the case of the BCS superconductivity [18].

Recently, Kitagawa *et al.* [14], showed that discrete-time quantum walks can realize topological phases in one and two dimensions in all the symmetry classes [21], [11] of the free-fermion systems given by quadratic Hamiltonians. In particular, they provide the quantum walk protocols that simulate representatives of all the topological phases, featured by the presence of robust symmetry-protected edge states (see also [12]). Quantum walks realizations are particularly useful because, in addition to the simplicity of their mathematical description, the parameters that define them can be easily controlled in the lab, allowing for the study of topological phase transitions and the corresponding edge states at the boundary between the different phases [13], [4].

We study topological features at finite temperatures of the Boltzmann-Gibbs thermal-like states of single-particle one-dimensional discrete-time topological quantum walks. We analyze the behaviour of the fidelity and the edge states,

and conclude that the effective temperature only smears out the topological features exhibited at zero temperature, without causing a thermal phase transition. We also show that an analogous conclusion can be drawn for the many-body systems studied in [25, 26].

This paper is organized as follows: First, we briefly describe the main topological features of quantum walks and their origin and present the respective protocols. For a detailed and complete analysis we refer to the original paper [14] and the subsequent review [12]. We also present the Boltzmann-Gibbs states we are going to use in the single-particle case of quantum walks, as well as for the many-body Hamiltonians and clarify the relationship between them, as well as the motivation for their use in different physical scenarios. In the next section, we present the analytical expressions for the fidelity for all cases, the corresponding numerical results and discuss the possibility of topological thermal-like transitions. In the same section, we also study the behaviour of edge states at finite temperature in these systems and we comment on the Uhlmann geometric phase and its relevance to probe topological phase transitions at finite temperatures. Finally, we summarize and discuss the results and point out possible directions of future work.

II. TOPOLOGICAL QUANTUM WALKS

We consider the so-called *split-step* one-dimensional discrete-time quantum walk introduced in [14]. A single step of the walk is given by the unitary

$$U(\theta_1, \theta_2) = T_1 R(\theta_2) T_0 R(\theta_1), \quad (1)$$

where the shift operators are:

$$T_c = \sum_x |x + (-1)^c\rangle \langle x| \otimes |c\rangle \langle c| + |x\rangle \langle x| \otimes |1 \oplus c\rangle \langle 1 \oplus c|, \quad (2)$$

with $c \in \{0, 1\}$ and \oplus being addition modulo 2, and the coin operators are $R(\theta) = e^{i\frac{\theta}{2}\vec{\alpha}\cdot\vec{\sigma}}$, where $\vec{\alpha}$ is a unit 3D vector, and $\vec{\sigma} = (\sigma_x, \sigma_y, \sigma_z)$ is the vector of Pauli matrices. The effective Hamiltonian that generates a single step, defined as $H_{\text{eff}} \equiv -i\Delta t^{-1} \log U$ (for simplicity, we take $\Delta t = 1$, for a single-step period of time), can, due to translational invariance, be written as:

$$\begin{aligned} H_{\text{eff}}(\theta_1, \theta_2) &= \sum_{k \in \mathcal{B}} H_k(\theta_1, \theta_2) \otimes |k\rangle \langle k| \\ &= \sum_{k \in \mathcal{B}} [E_k(\theta_1, \theta_2) \vec{n}_k(\theta_1, \theta_2) \cdot \vec{\sigma}] \otimes |k\rangle \langle k|, \end{aligned} \quad (3)$$

where \mathcal{B} is the first Brillouin zone, $E_k \geq 0$ and \vec{n}_k are 3D unit vectors (for simplicity, we omit the θ -dependences). The eigenstates are given by $H_k|\pm\vec{n}_k\rangle = \pm E_k|\pm\vec{n}_k\rangle$, thus forming two energy bands $\{\pm E_k, k \in \mathcal{B}\}$. This type of Hamiltonians exhibit topological phases in the presence of certain symmetries, namely time-reversal, particle-hole and the chiral/sub-lattice symmetry (see [14] and the references therein). The symmetry classes we study in this paper (BDI and AIII in the Cartan classification) are chiral with a \mathbb{Z} invariant. This implies that \vec{n}_k , which defines the quantization axis for each quasi-momentum k , is restricted to lie on a great circle of the Bloch sphere, determined by $\vec{\alpha}$ and θ_1 . The number of times that \vec{n}_k winds around the origin, as k ranges within the first Brillouin zone \mathcal{B} , is the *winding number* of the map between the two circles. This is exactly what gives rise to the topological features of the quantum walk. The other symmetries are then determined by the choice of $\vec{\alpha}$ and/or by doubling the coin degree of freedom (for details, see [14] and [12]). For each different symmetry class we study, we fix the value of θ_1 and vary θ_2 , so from now on, we consider $H_{\theta_1}^{\text{eff}}(\theta) \equiv H^{\text{eff}}(\theta_1, \theta)$ (see Appendix, Table I, for the specific protocols). By additionally varying θ along the line of the walk, it is possible to create a domain wall that separates two different phases, centred at the origin of the quantum walk, where the aforementioned edge states lie.

III. BOLTZMANN-GIBBS DENSITY OPERATORS

We consider two types of Boltzmann-Gibbs-like states for the above described single-particle quantum walk. The first one is the standard thermal state:

$$\begin{aligned} \rho^{(0)} &= \frac{e^{-\beta H}}{\mathcal{Z}} = \frac{1}{\mathcal{Z}} e^{-\beta(\sum_{k \in \mathcal{B}} H_k \otimes |k\rangle \langle k|)} \\ &= \frac{1}{\mathcal{Z}} \sum_{k \in \mathcal{B}} e^{-\beta H_k} \otimes |k\rangle \langle k|, \end{aligned} \quad (4)$$

where $Z = \text{Tr}e^{-\beta H}$, while the second is:

$$\rho^{(1)} = \frac{1}{\Omega} \sum_{k \in \mathcal{B}} \frac{e^{-\beta H_k}}{Z_k} \otimes |k\rangle\langle k| = \frac{1}{\Omega} \sum_{k \in \mathcal{B}} \rho_k \otimes |k\rangle\langle k|, \quad (5)$$

where $Z_k = \text{Tr}e^{-\beta H_k}$ and $\Omega = \sum_k 1$ is the volume of the k -space. Note that by tracing out the momenta, the state $\rho^{(0)}$ remains to be of the Boltzmann-Gibbs form (it is ‘‘globally’’, with respect to k , thermal-like), while $\rho^{(1)}$ is not – only by measuring the momenta, the state collapses to a ‘‘local’’ Boltzmann-Gibbs form $\rho_k = e^{-\beta H_k}/Z_k$. Notice also that $Z = \sum_k Z_k$. The difference between $\rho^{(0)}$ and $\rho^{(1)}$ can become even more clear if we look at their asymptotic behaviours. Namely, when $\beta \rightarrow +\infty$

$$\rho^{(0)} \rightarrow \frac{1}{|M|} \sum_{k \in M} |-\vec{n}_k\rangle\langle -\vec{n}_k| \otimes |k\rangle\langle k|, \quad (6)$$

where $M = \{k_* \in \mathcal{B} : E(k_*) = \max_{k \in \mathcal{B}} E(k)\}$ is the set of momenta that minimize the lower band dispersion, while

$$\rho^{(1)} \rightarrow \frac{1}{\Omega} \sum_{k \in \mathcal{B}} |-\vec{n}_k\rangle\langle -\vec{n}_k| \otimes |k\rangle\langle k|, \quad (7)$$

which is a statistical mixture of the *entire* lower band of the Hamiltonian.

The above states are projections onto the single-particle sector of many-body states associated to translationally invariant free-fermion systems. The first state is the canonical ensemble given by,

$$\varrho^{(0)} = \frac{e^{-\beta \mathcal{H}}}{\text{Tr}(e^{-\beta \mathcal{H}})},$$

where \mathcal{H} is given by the sum over the momenta of quadratic Hamiltonians

$$\mathcal{H} = \sum_k \Psi_k^\dagger H_k \Psi_k, \quad (8)$$

where, for each k , Ψ_k denotes a vector of fermion annihilation operators (note that \mathcal{H} conserves the particle number and its action on the whole Hilbert space is determined by the action on the single-particle sector). This state maximizes the von Neumann entropy, subject to the constraint:

$$\langle \mathcal{H} \rangle = \text{const}. \quad (9)$$

The second one appears when one maximizes the von Neumann entropy, subject to two constraints: the above mentioned energy constraint, as well as the constraint on the average number of particles for each momentum k ,

$$\langle n_k \rangle = \langle \Psi_k^\dagger \Psi_k \rangle = \text{const}. \quad (10)$$

The state is of the form:

$$\varrho^{(1)} = \frac{e^{-\beta \mathcal{O}}}{\text{Tr}(e^{-\beta \mathcal{O}})},$$

where $\mathcal{O} = \sum_k \mathcal{O}_k = \sum_k \mathcal{H}_k - \mu_k n_k$, with μ_k being a momentum dependent chemical potential. For details concerning the derivation of these states or, more generally, states maximizing the von Neumann entropy subject to constraints, cf. the appendix of [24].

It is important to clarify the relation between single-particle density matrices and the corresponding many-body operators, since the quantum walk we are performing concerns only the single-particle sector. Let us consider a collection of fermion creation and annihilation operators $\{\psi_{k\sigma}, \psi_{k\sigma}^\dagger : k \in \mathcal{B}, \sigma \in \{\uparrow, \downarrow\}\}$ and form the spinors $\Psi_k = (\psi_{k\uparrow}, \psi_{k\downarrow})^T$. Then, there exists a bijection between single-particle and quadratic many-body Hamiltonians, given by

$$H_k \leftrightarrow \mathcal{H}_k = \Psi_k^\dagger H_k \Psi_k, \quad (11)$$

where the left arrow represents the aforementioned projection onto the single-particle sector, thus inducing the corresponding bijections between the Boltzmann-Gibbs states:

$$\begin{aligned}\rho^{(0)} \leftrightarrow \varrho^{(0)} &= \frac{1}{\mathcal{Z}^{(0)}} \prod_{k \in \mathcal{B}} \exp(-\beta \Psi_k^\dagger H_k \Psi_k), \\ \rho^{(1)} \leftrightarrow \varrho^{(1)} &= \frac{1}{\mathcal{Z}^{(1)}} \prod_{k \in \mathcal{B}} \exp[-\beta(\Psi_k^\dagger H_k \Psi_k - \mu_k \Psi_k^\dagger \Psi_k)],\end{aligned}\tag{12}$$

where $\mu_k = -(1/\beta) \log(Z_k)$ is the chemical potential for momentum k which, in this case, coincides with the Helmholtz free energy associated to momentum k and $\mathcal{Z}^{(0)}, \mathcal{Z}^{(1)}$ are the corresponding partition functions.

IV. THE RESULTS: FIDELITY, EDGE STATES AND THE UHLMANN PHASE

As mentioned in the Introduction, the fidelity is an information-theoretical measure of the distinguishability between two quantum states ρ and σ , defined as: $F(\rho, \sigma) \equiv \text{Tr} \sqrt{\sqrt{\rho} \sigma \sqrt{\rho}}$. Whenever there is a phase transition the density matrix describing the system changes significantly and, therefore, a sudden drop of the fidelity signals out this change. In our fidelity analysis we will consider two states separated in the space of parameters (β^{-1}, θ) by a small (“infinitesimal”) displacement: namely $F(\rho, \rho')$, where prime denotes the infinitesimally close parameters. Table IV summarizes the expressions for the fidelity for the Boltzmann-Gibbs states considered. The details concerning the derivation can be found in Appendix. The numerical results for the representative of the class BDI are given in Fig. 1. The results for the representative of the class AIII are qualitatively similar and, thus, we omit them. Below, we discuss both the analytic and the numerical results.

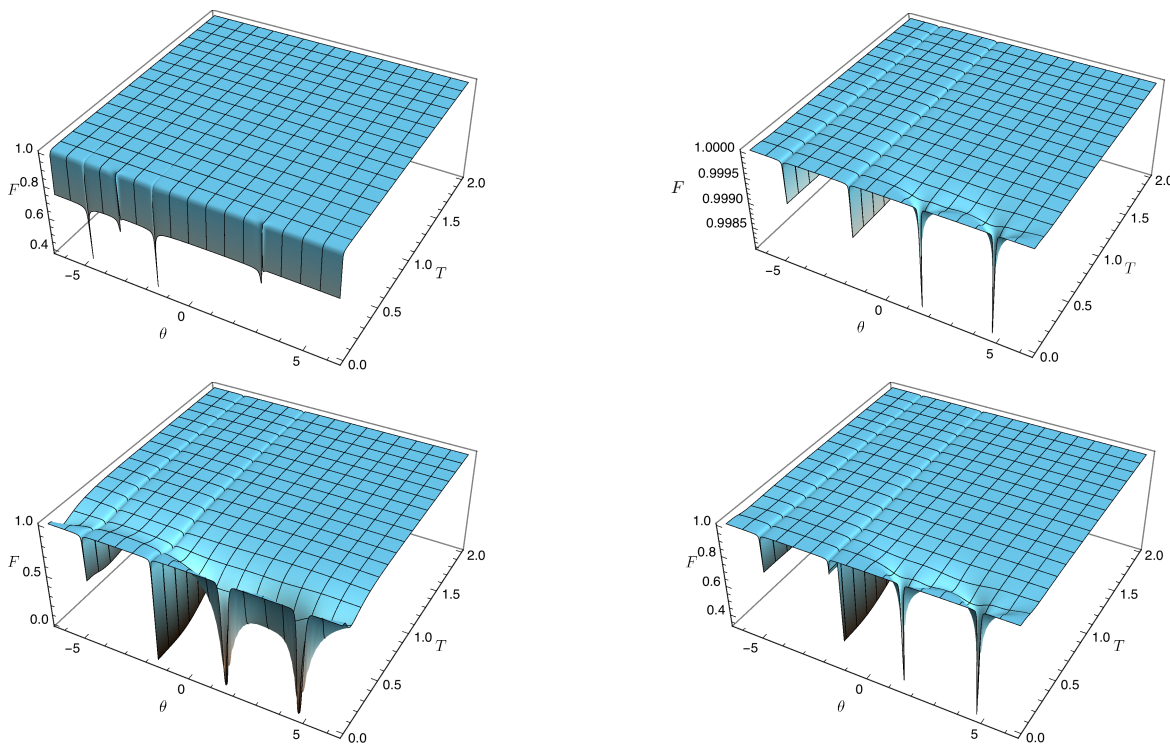
A unique feature of periodically driven systems is that both energies $E_k = 0$ and $E_k = \pi$ correspond to a closed gap (the difference between the two energy levels $\pm E_k$ becomes zero modulo 2π). This special feature of quantum walks, due to periodicity, yields a surprising result in our analysis. In the fidelity study we perform, we observe a different behaviour of the gap closing points with temperature, depending on whether they correspond to $E_k = 0$ (the two points with $\theta > 0$) or $E_k = \pi$ energy (the two points with $\theta < 0$). Whenever the gap closes, the vector \vec{n} is ill-defined (for its specific form, see [14]), but the way the fidelity behaves will be different due to its dependence on the entire energy spectrum. For the case of $E_k = 0$, the fidelity signals two isolated zero-temperature points of quantum phase transitions, corresponding to $\theta = \pi/2, 3\pi/2$. As the temperature increases, the fidelity is no longer signalling a phase transition and this is due to the dependence on the hyperbolic sine of E_k , which vanishes for $E_k = 0$ (see Table IV), thus eliminating the $\vec{n} \cdot \vec{n}'$ term carrying the relevant topological features. The significance of these points of the zero-temperature quantum phase transitions on the system in the low-temperature regime, and the existence of possible crossovers, remain an open question and requires further investigation. In contrast to that, for the $E_k = \pi$ gap closing points, the phase transition lines survive with temperature, hence revealing a “finite-temperature quantum phase transition” (a phase transition driven solely by the Hamiltonian’s parameter(s), and not the temperature). Again, this can be understood through the dependence on E_k via hyperbolic functions which take finite values for $E_k = \pi$, thus maintaining the dependence on $\vec{n} \cdot \vec{n}'$.

Notice that for $\rho^{(0)}$ the qualitative behaviour is different from the other three cases: the fidelity does not drop for $T = 0$ and $\theta = \pi/2, 3\pi/2$, while it does for two new $T = 0$ points at $\theta = \pm\pi$. The first difference is due to the fact that the zero temperature limit of $\rho^{(0)}$ projects only onto M given by the points of minimum energy $-E_k = -\pi$, see Eq. (6). Thus, the fidelity $F(\rho^{(0)}, \rho'^{(0)})$ does not see the critical momentum at which the gap closes at zero energy, which is above the lowest mode. The abrupt change of the fidelity at the points where $\theta = \pm\pi$ is the consequence of the enhanced zero-temperature ground state distinguishability due to the fact that E_k becomes constant and independent of k , i.e., the zero-temperature state projects onto the whole Brillouin zone ($M(\theta = \pm\pi) = \mathcal{B}$). While the numerical results for the representatives for the two classes BDI and AIII are qualitatively similar, the zero-temperature fidelity corresponding to the $\rho^{(0)}$ states for the AIII representative only exhibits drops in the gap closing points ($-E_k = -\pi$), as the spectrum is always non-trivially k -dependent.

We now proceed to present and discuss the results regarding edge states. The bulk-to-boundary principle predicts the existence of edge states on the boundary between two distinct topological phases. These states are symmetry protected, in the sense that they are robust against perturbations of the Hamiltonian which respect the symmetries of the system. In the case of pure states, quantum walks realize the aforementioned principle as shown in [14]. To this end, the authors introduce a spatial dependence on the parameter θ of the Hamiltonian in such a way that a phase boundary is created. The edge states are then observed by evolving the walk *in time* from the initial state localized at the phase boundary: the probability to find the system in the initial position keeps being (considerably)

Boltzmann-Gibbs state	Fidelity
$\rho^{(0)}$	$\frac{\sum_k \sqrt{2(1+\cosh(E_k/2T) \cosh(E'_k/2T')+\sinh(E_k/2T) \sinh(E'_k/2T')\vec{n}_k \cdot \vec{n}'_k)}}{\sqrt{\sum_k 2 \cosh(E_k/2T) \sum_k 2 \cosh(E'_k/2T')}}}$
$\rho^{(1)}$	$\sum_k \frac{\sqrt{2(1+\cosh(E_k/2T) \cosh(E'_k/2T')+\sinh(E_k/2T) \sinh(E'_k/2T')\vec{n}_k \cdot \vec{n}'_k)}}{\sqrt{2 \cosh(E_k/2T) 2 \cosh(E'_k/2T')}}}$
$\varrho^{(0)}$	$\prod_k \frac{2+\sqrt{2(1+\cosh(E_k/2T) \cosh(E'_k/2T')+\sinh(E_k/2T) \sinh(E'_k/2T')\vec{n}_k \cdot \vec{n}'_k)}}{\sqrt{[2+2 \cosh(E_k/2T)][2+2 \cosh(E'_k/2T')]}}$
$\varrho^{(1)}$	$\prod_k \frac{1+\frac{1+\cosh(E_k/2T) \cosh(E'_k/2T')+\sinh(E_k/2T) \sinh(E'_k/2T')\vec{n}_k \cdot \vec{n}'_k}{\sqrt{\cosh(E_k/2T) \cosh(E'_k/2T')}}+\frac{1}{4 \cosh(E_k/2T) \cosh(E'_k/2T')}}{\sqrt{[2+(2 \cosh(E_k/2T))^{-2}][2+(2 \cosh(E'_k/2T'))^{-2}]}}$

TABLE I: Fidelity formulae for the Boltzmann-Gibbs states considered.

FIG. 1: Fidelity for the single-particle states $\rho^{(0)}$ (top left) and $\rho^{(1)}$ (top right), and the many-body states $\varrho^{(0)}$ (bottom left) and $\varrho^{(1)}$ (bottom right), for the BDI symmetry class. $\delta\theta = \theta' - \theta = 0.01$ and $\delta T = T' - T = 0.01$.

higher than for the rest of the line. Instead, in our case, we are interested in probing the robustness of the edge states with respect to temperature. Therefore, we study an ensemble of the Boltzmann-Gibbs type which corresponds to a stationary state of such walk with the position-dependent coin operation, parameterized by its temperature β^{-1} . This stationary state appears naturally if one looks at the von Neumann evolution equation for the density matrix and imposes the stationarity condition. By diagonalizing H_{eff} we obtain the localized states which can either have quasi-energy 0 or π . Written in terms of an eigenbasis $\{|\alpha\rangle\}$ the effective Hamiltonian is $H_{\text{eff}} = \sum_{\alpha} \varepsilon_{\alpha} |\alpha\rangle\langle\alpha|$. At zero temperature, the edge state gets the major contribution to the probability distribution. As temperature increases, the edge states are smeared out. Since the presence of an edge state is a clear manifestation of the topological order of a system at $T = 0$ then, the fact that it does not disappear for high temperatures, but it is rather smeared out, shows explicitly that the topological nature of the system is preserved in agreement with the fidelity analysis for the $E_k = \pi$ gap-closing points.

We complete this section with a brief discussion on the relevance of the Uhlmann phase to inferring a phase

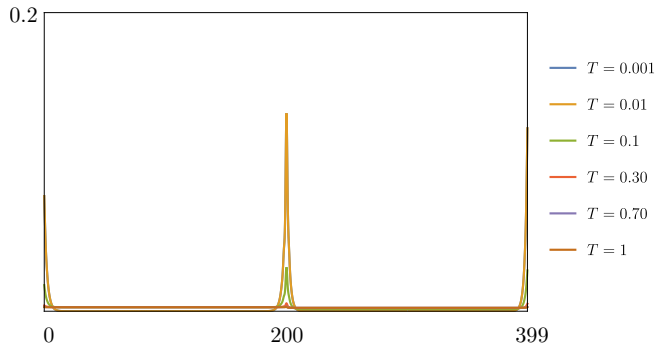


FIG. 2: Position probability distribution of the quantum walk as a function of the sites, $\text{Tr}(e^{-H/T}|x\rangle\langle x|)/Z$. The Hamiltonian H is obtained by varying θ along x through a step-like function, as in [14]. The domain-wall is centered in the middle of the line. Periodic boundary conditions are taken, hence the edge state at the boundary.

transition driven by temperature. In Ref. [26] the authors introduce the Uhlmann “critical” temperature T_U above which the Uhlmann holonomy becomes trivial, and analyze its physical meaning associated to the existence of a “critical momentum” k_c below which the Uhlmann phase is trivial, while above it the phase becomes π . Note that k_c depends on temperature and is different from the gap-closing momenta considered in this paper, which signal out the points of zero-temperature quantum phase transitions (these points are also indicated by the Berry holonomy, the zero-temperature limit of the Uhlmann holonomy). However, our fidelity analysis reveals that for $T > 0$ there exist no thermal phase transitions (i.e., no temperature-driven phase transitions), as pointed out by Andersson *et al.* on the example of the Kitaev model [2]. The non-existence of thermal phase transitions is also confirmed by the behaviour of the edge states, which are gradually smeared out with the temperature increase, as also pointed out by the authors of [26]. Note also that the Uhlmann holonomy studied in [26] does not refer to a genuine multi-particle case, as it is obtained for the family of matrices $\{\rho_k = e^{-\beta H_k}/Z_k : k \in \mathcal{B}\}$, with the momentum space as the base space, associated to the single-particle state $\rho^{(1)}$ given by equation (5). The connection between the Uhlmann parallel transport and the finite-temperature phase transitions has been studied before on the example of the BCS superconductivity [18]. Instead of “partial” states ρ_k over the momentum space, in [18] the authors studied the overall quantum states over the parameter space (including the temperature) as a base space. It was shown that the “Uhlmann factor” U , given by $\sqrt{\rho}\sqrt{\rho'} = |\sqrt{\rho}\sqrt{\rho'}|U$, quantifies the difference between the eigen-bases of the two states ρ and ρ' , taken in two close points of the parameter space, thus quantifying the distinguishability between the two states as well. Its abrupt departure from the identity clearly marked the line of the thermal phase transition (see [18] for more details).

Conclusions and Outlook

We derived an analytic expression for the fidelity between two Boltzmann-Gibbs states for quantum walk representatives of topological phases for the chiral symmetric classes BDI and AIII. For the systems considered, we have seen that fidelity is detecting the points where the Bloch vector is ill-defined, which is equivalent to the closure of the quasi-energy gap. Furthermore, fidelity is capturing the topological phase transitions, since in our case the phase diagram is such that the closure of the gap always means the change from a trivial phase to a non-trivial one, and vice-versa. Our results show the non existence of thermal-like phase transitions in two ways: through the fidelity analysis and through the behaviour of the edge states appearing on the phase boundary.

We remarked the fact that the Uhlmann geometric phase is not inferring a thermal phase transition. We would also like to stress that the Uhlmann geometric phase is only part of the information contained in the holonomy associated to the Uhlmann connection. In reality, this holonomy, as a function of temperature, is smooth, and, hence, no phase transition-like phenomenon is expected.

Finally, we point out possible future lines of research. First, the same study could be applied to the rest of the symmetry classes in one and two dimensions using the protocols introduced in [14]. Then, a question that naturally arises is what kind of realistic noise effects could give rise to these single-particle Boltzmann-Gibbs states $\rho^{(0)}$ and $\rho^{(1)}$. Another direction entails the generalization of the above approach to two (or more) dimensional quantum walks. Finally, one could also study topological phase transitions in the realm of multi-particle quantum walks at zero and finite temperatures.

Acknowledgements

B. M. and C. V. acknowledge the support from DP-PMI and FCT (Portugal) through the grants SFRH/BD/52244/2013 and PD/BD/52652/2014, respectively. N. P. acknowledges the IT project QbigD funded by FCT PEst-OE/EEI/LA0008/2013, UID/EEA/50008/2013 and the Confident project PTDC/EEI-CTP/4503/2014. Support from FCT (Portugal) through Grant UID/CTM/04540/2013 is also acknowledged.

-
- [1] Damian F. Abasto, Alioscia Hamma, and Paolo Zanardi. Fidelity analysis of topological quantum phase transitions. *Phys. Rev. A*, 78:010301, Jul 2008.
 - [2] Ole Andersson, Ingemar Bengtsson, Marie Ericsson, and Erik Sjöqvist. Geometric phases for mixed states of the kitaev chain. *Philosophical Transactions of the Royal Society of London A: Mathematical, Physical and Engineering Sciences*, 374(2068), 2016.
 - [3] Yoichi Ando. Topological insulator materials. *Journal of the Physical Society of Japan*, 82(10):102001, 2013.
 - [4] Sonia Barkhofen, Thomas Nitsche, Fabian Elster, Lennart Lorz, Aurel Gabris, Igor Jex, and Christine Silberhorn. Measuring topological invariants and protected bound states in disordered discrete time quantum walks. *arXiv:1606.00299v1*.
 - [5] M. V. Berry. Quantal phase factors accompanying adiabatic changes. *Proceedings of the Royal Society of London A: Mathematical, Physical and Engineering Sciences*, 392(1802):45–57, 1984.
 - [6] Shi-Jian Gu, Ho-Man Kwok, Wen-Qiang Ning, and Hai-Qing Lin. Fidelity susceptibility, scaling, and universality in quantum critical phenomena. *Phys. Rev. B*, 77:245109, Jun 2008.
 - [7] Gábor B. Halász and Alioscia Hamma. Probing topological order with rényi entropy. *Phys. Rev. A*, 86:062330, Dec 2012.
 - [8] F. D. M. Haldane. Model for a quantum hall effect without landau levels: Condensed-matter realization of the “parity anomaly”. *Phys. Rev. Lett.*, 61:2015–2018, Oct 1988.
 - [9] A. Hamma, W. Zhang, S. Haas, and D. A. Lidar. Entanglement, fidelity, and topological entropy in a quantum phase transition to topological order. *Phys. Rev. B*, 77:155111, Apr 2008.
 - [10] Alioscia Hamma, Radu Ionicioiu, and Paolo Zanardi. Ground state entanglement and geometric entropy in the kitaev model. *Physics Letters A*, 337(1–2):22 – 28, 2005.
 - [11] Alexei Kitaev. Periodic table for topological insulators and superconductors. *AIP Conference Proceedings*, 1134(1), 2009.
 - [12] Takuya Kitagawa. Topological phenomena in quantum walks: elementary introduction to the physics of topological phases. *Quantum Information Processing*, 11(5):1107–1148, 2012.
 - [13] Takuya Kitagawa, Matthew A Broome, Alessandro Fedrizzi, Mark S Rudner, Erez Berg, Ivan Kassal, Alán Aspuru-Guzik, Eugene Demler, and Andrew G White. Observation of topologically protected bound states in photonic quantum walks. *Nature communications*, 3:882, 2012.
 - [14] Takuya Kitagawa, Mark S. Rudner, Erez Berg, and Eugene Demler. Exploring topological phases with quantum walks. *Phys. Rev. A*, 82:033429, Sep 2010.
 - [15] Dalimil Mazáč and Alioscia Hamma. Topological order, entanglement, and quantum memory at finite temperature. *Annals of Physics*, 327(9):2096 – 2111, 2012.
 - [16] T. P. Oliveira and P. D. Sacramento. Entanglement modes and topological phase transitions in superconductors. *Phys. Rev. B*, 89:094512, Mar 2014.
 - [17] N. Paunković, P. D. Sacramento, P. Nogueira, V. R. Vieira, and V. K. Dugaev. Fidelity between partial states as a signature of quantum phase transitions. *Phys. Rev. A*, 77:052302, May 2008.
 - [18] Nikola Paunković and Vitor Rocha Vieira. Macroscopic distinguishability between quantum states defining different phases of matter: Fidelity and the uhlmann geometric phase. *Phys. Rev. E*, 77:011129, Jan 2008.
 - [19] A. Rivas, O. Viyuela, and M. A. Martin-Delgado. Density-matrix chern insulators: Finite-temperature generalization of topological insulators. *Phys. Rev. B*, 88:155141, Oct 2013.
 - [20] Shinsei Ryu and Yasuhiro Hatsugai. Topological origin of zero-energy edge states in particle-hole symmetric systems. *Phys. Rev. Lett.*, 89:077002, Jul 2002.
 - [21] Andreas P. Schnyder, Shinsei Ryu, Akira Furusaki, and Andreas W. W. Ludwig. Classification of topological insulators and superconductors in three spatial dimensions. *Phys. Rev. B*, 78:195125, Nov 2008.
 - [22] D. J. Thouless, M. Kohmoto, M. P. Nightingale, and M. den Nijs. Quantized hall conductance in a two-dimensional periodic potential. *Phys. Rev. Lett.*, 49:405–408, Aug 1982.
 - [23] A. Uhlmann. On berry phases along mixtures of states. *Annalen der Physik*, 501(1):63–69, 1989.
 - [24] VR Vieira. Quantum information and phase transitions: Fidelity and state distinguishability. 213(1), 2010.
 - [25] O. Viyuela, A. Rivas, and M. A. Martin-Delgado. Two-dimensional density-matrix topological fermionic phases: Topological uhlmann numbers. *Phys. Rev. Lett.*, 113:076408, Aug 2014.
 - [26] O. Viyuela, A. Rivas, and M. A. Martin-Delgado. Uhlmann phase as a topological measure for one-dimensional fermion systems. *Phys. Rev. Lett.*, 112:130401, Apr 2014.
 - [27] X. G. Wen. Gapless boundary excitations in the quantum hall states and in the chiral spin states. *Phys. Rev. B*, 43:11025–11036, May 1991.
 - [28] Paolo Zanardi, Paolo Giorda, and Marco Cozzini. Information-theoretic differential geometry of quantum phase transitions. *Phys. Rev. Lett.*, 99:100603, Sep 2007.

- [29] Paolo Zanardi and Nikola Paunković. Ground state overlap and quantum phase transitions. *Phys. Rev. E*, 74:031123, Sep 2006.
- [30] Bei Zeng, Xie Chen, Duan-Lu Zhou, and Xiao-Gang Wen. *Quantum Information meets Quantum Matter—From Quantum Entanglement to Topological Phase in Many-Body Systems*,. arxiv.org/abs/1508.02595.
- [31] Jian-Hui Zhao and Huan-Qiang Zhou. Singularities in ground-state fidelity and quantum phase transitions for the kitaev model. *Phys. Rev. B*, 80:014403, Jul 2009.

Appendix

Quantum walk protocols

Class	TRS	PHS	CS	Protocol	Parameters	w
	$\mathcal{T} = \Gamma_{\theta_1} \mathcal{P}$	$\mathcal{P} = \mathcal{K}$	$\Gamma_{\theta_1} = \exp(-i\pi \vec{A}_{\theta_1} \cdot \vec{\sigma}/2)$	$T_{\downarrow} R_y(\theta_2) T_{\uparrow} R_y(\theta_1)$	$\theta_1 = -\pi/2, \theta_2 = 3\pi/4$	$w = 0$
BDI	$\mathcal{T}^2 = 1$	$\mathcal{P}^2 = 1$	$\Gamma^2 = 1$		$\theta_1 = -\pi/2, \theta_2 = \pi/4$	$w = 1$
AIII	Absent	Absent	$\Gamma_{\theta_1}^{\alpha} = \exp(-i\pi \vec{A}_{\theta_1}^{\alpha} \cdot \vec{\sigma}/2)$	$T_{\downarrow} R_{\alpha}(\theta_2) T_{\uparrow} R_{\alpha}(\theta_1)$	$\theta_1 = \pi/2, \theta_2 = 3\pi/4$	$w = 0$
			$\Gamma^2 = 1$		$\theta_1 = \pi/2, \theta_2 = \pi/4$	$w = 1$

TABLE II: Chiral Symmetric Classes in 1D with a \mathbb{Z} invariant and the respective quantum walk protocols that simulate them. \mathcal{K} stands for complex conjugation, $\vec{\alpha}$ is the vector $1/\sqrt{2}(0, 1, 1)$ and the \vec{A} vectors are $\vec{A}_{\theta_1} = [\cos(\theta_1/2), 0, \sin(\theta_1/2)]$ and $\vec{A}_{\theta_1}^{\alpha} = [\cos(\theta_1/2), -1/\sqrt{2}\sin(\theta_1/2), 1/\sqrt{2}\sin(\theta_1/2)]$, respectively. We include the values of the parameters that correspond to distinct topological phases, described by different winding numbers w .

Analytic derivation of the closed expression for the fidelity

If ρ and ρ' are two states which are not normalized, the fidelity is given by

$$F(\rho, \rho') = \text{Tr} \sqrt{\sqrt{\rho} \rho' \sqrt{\rho}}. \quad (13)$$

We consider $\rho = \exp(-\beta H)$ and $\rho' = \exp(-\beta' H')$. At the end of the calculation one must, of course, normalize the expression appropriately. We wish to find closed expressions for the four possible density matrices we present in the main text. In order to do that we will proceed by finding e^C , such that

$$e^A e^B e^A = e^C,$$

for $A = -\beta H$, $B = -\beta' H'$ and, ultimately, take the square root of the result. The previous equation is equivalent to

$$e^A e^B = e^C e^{-A}. \quad (14)$$

The Hamiltonians H and H' are taken to be of the form $\vec{h} \cdot \vec{\sigma}$, and thus we can write

$$e^A = a_0 + \vec{a} \cdot \vec{\sigma},$$

$$e^B = b_0 + \vec{b} \cdot \vec{\sigma},$$

$$e^C = c_0 + \vec{c} \cdot \vec{\sigma},$$

where all the coefficients are real, with the following constraints:

$$\begin{cases} 1 = \det e^A = a_0^2 - \vec{a}^2 \\ 1 = \det e^B = b_0^2 - \vec{b}^2 \\ 1 = \det e^C = c_0^2 - \vec{c}^2 \end{cases}, \quad (15)$$

which are equivalent to $\text{Tr} A = \text{Tr} B = \text{Tr} C = 0$, since Pauli matrices are traceless. Let us proceed by expanding the LHS and the RHS of Eq.(14),

$$\begin{aligned} (a_0 + \vec{a} \cdot \vec{\sigma})(b_0 + \vec{b} \cdot \vec{\sigma}) &= (c_0 + \vec{c} \cdot \vec{\sigma})(a_0 - \vec{a} \cdot \vec{\sigma}) \Leftrightarrow \\ a_0 b_0 + a_0 \vec{b} \cdot \vec{\sigma} + \vec{a} \cdot \vec{\sigma} b_0 + (\vec{a} \cdot \vec{\sigma})(\vec{b} \cdot \vec{\sigma}) &= c_0 a_0 - c_0 \vec{a} \cdot \vec{\sigma} + \vec{c} \cdot \vec{\sigma} a_0 - (\vec{c} \cdot \vec{\sigma})(\vec{a} \cdot \vec{\sigma}) \Leftrightarrow \\ a_0 b_0 + a_0 \vec{b} \cdot \vec{\sigma} + \vec{a} \cdot \vec{\sigma} b_0 + \vec{a} \cdot \vec{b} + i(\vec{a} \times \vec{b}) \cdot \vec{\sigma} &= c_0 a_0 - c_0 \vec{a} \cdot \vec{\sigma} + \vec{c} \cdot \vec{\sigma} a_0 - \vec{c} \cdot \vec{a} - i(\vec{c} \times \vec{a}) \cdot \vec{\sigma}. \end{aligned}$$

Now, collecting terms in 1, $\vec{\sigma}$ and $i\vec{\sigma}$, we get a system of linear equations on c_0 and \vec{c} ,

$$\begin{cases} a_0 b_0 + \vec{a} \cdot \vec{b} - a_0 c_0 + \vec{a} \cdot \vec{c} = 0 \\ a_0 \vec{b} + b_0 \vec{a} + \vec{a} c_0 - a_0 \vec{c} = 0 \\ \vec{a} \times \vec{b} - \vec{a} \times \vec{c} = 0 \end{cases} . \quad (16)$$

The third equation from (16) can be written as $\vec{a} \times (\vec{b} - \vec{c}) = 0$, whose solution is given by $\vec{c} = \vec{b} + \lambda \vec{a}$, where λ is a real number. This means that the solution depends only on two real parameters: c_0 and λ . Hence, we are left with a simpler system given by,

$$\begin{cases} a_0 b_0 + \vec{a} \cdot \vec{b} - a_0 c_0 + \vec{a} \cdot (\vec{b} + \lambda \vec{a}) = 0 \\ a_0 \vec{b} + b_0 \vec{a} + \vec{a} c_0 - a_0 (\vec{b} + \lambda \vec{a}) = 0 \end{cases} . \quad (17)$$

Or,

$$\begin{cases} a_0 c_0 - \lambda \vec{a}^2 = a_0 b_0 + 2\vec{a} \cdot \vec{b} \\ (a_0 \lambda - c_0) \vec{a} = b_0 \vec{a} \end{cases} . \quad (18)$$

In matrix form, the above system of equations can be written as

$$\begin{bmatrix} a_0 & -\vec{a}^2 \\ -1 & a_0 \end{bmatrix} \begin{bmatrix} c_0 \\ \lambda \end{bmatrix} = \begin{bmatrix} a_0 b_0 + 2\vec{a} \cdot \vec{b} \\ b_0 \end{bmatrix} \quad (19)$$

Inverting the matrix, we get

$$\begin{aligned} \begin{bmatrix} c_0 \\ \lambda \end{bmatrix} &= \frac{1}{a_0^2 - \vec{a}^2} \begin{bmatrix} a_0 & \vec{a}^2 \\ 1 & a_0 \end{bmatrix} \begin{bmatrix} a_0 b_0 + 2\vec{a} \cdot \vec{b} \\ b_0 \end{bmatrix} \\ &= \begin{bmatrix} (2a_0^2 - 1)b_0 + 2a_0 \vec{a} \cdot \vec{b} \\ 2(a_0 b_0 + \vec{a} \cdot \vec{b}) \end{bmatrix}, \end{aligned}$$

where we used the constraints (15). Because of the constraint, c_0 and λ are not independent, namely, $e^C = c_0 + (\vec{b} + \lambda \vec{a}) \cdot \vec{\sigma}$, and we get

$$c_0^2 - (\vec{b} + \lambda \vec{a})^2 = c_0^2 - \vec{b}^2 - 2\lambda \vec{a} \cdot \vec{b} - \vec{a}^2 = 1.$$

Now we want to make $A = -\beta H/2 \equiv -\xi \vec{x} \cdot \vec{\sigma}/2$ and $B = -\beta' H' \equiv -\zeta \vec{y} \cdot \vec{\sigma}$, with $\vec{x}^2 = \vec{y}^2 = 1$ and ξ and ζ real parameters, meaning,

$$a_0 = \cosh(\xi/2) \text{ and } \vec{a} = -\sinh(\xi/2) \vec{x}, \quad (20)$$

$$b_0 = \cosh(\zeta) \text{ and } \vec{b} = -\sinh(\zeta) \vec{y}. \quad (21)$$

If we write $C = \rho \vec{z} \cdot \vec{\sigma}$ (because the product of matrices with determinant 1 has to have determinant 1, it has to be of this form),

$$\begin{aligned} c_0 &= \cosh(\rho) \\ &= (2a_0^2 - 1)b_0 + 2a_0 \vec{a} \cdot \vec{b} \\ &= (2 \cosh^2(\xi/2) - 1) \cosh(\zeta) + 2 \cosh(\xi/2) \sinh(\xi/2) \sinh(\zeta) \vec{x} \cdot \vec{y} \\ &= \cosh(\xi) \cosh(\zeta) + \sinh(\xi) \sinh(\zeta) \vec{x} \cdot \vec{y}. \end{aligned}$$

For all the expressions concerning fidelity, we wish to compute $\text{tr}(e^{C/2}) = 2 \cosh(\rho/2)$. If we use the formula $\cosh(\rho/2) = \sqrt{(1 + \cosh(\rho))/2}$, we obtain,

$$\text{tr}(e^{C/2}) = 2 \sqrt{\frac{(1 + \cosh(\xi) \cosh(\zeta) + \sinh(\xi) \sinh(\zeta) \vec{x} \cdot \vec{y})}{2}},$$

Hence,

$$\text{tr}(\sqrt{e^{-\beta H/2} e^{-\beta' H'} e^{-\beta H/2}}) = 2\sqrt{\frac{(1 + \cosh(\beta\Delta) \cosh(\beta'\Delta') + \sinh(\beta\Delta) \sinh(\beta'\Delta') \vec{n} \cdot \vec{n}')}{2}}.$$

To be able to compute all the fidelities, we will just need the following expression relating the traces of quadratic many-body fermion Hamiltonians (preserving the number operator) and the single-particle sector Hamiltonian obtained by projection:

$$\text{Tre}^{-\beta \mathcal{H}} = \text{Tre}^{-\beta \Psi^\dagger H \Psi} = \det(I + e^{-\beta H}). \quad (22)$$

From the previous results, it is straightforward to derive the following formulae for the fidelities concerning all the *normalized* states discussed in the main text:

Single-Body

$$\begin{aligned} F(\rho^{(0)}, \rho'^{(0)}) &= \frac{\sum_{k \in \mathcal{B}} \text{Tr}(e^{-C_k/2})}{\sqrt{\sum_{k \in \mathcal{B}} \text{Tr}(e^{-\beta H_k}) \sum_{k \in \mathcal{B}} \text{Tr}(e^{-\beta' H'_k})}} \\ &= \frac{\sum_{k \in \mathcal{B}} \sqrt{2(1 + \cosh(E_k/2T) \cosh(E'_k/2T') + \sinh(E_k/2T) \sinh(E'_k/2T') \vec{n}_k \cdot \vec{n}'_k)}}{\sqrt{\sum_{k \in \mathcal{B}} 2 \cosh(E_k/2T) \sum_{k \in \mathcal{B}} 2 \cosh(E'_k/2T')}} \end{aligned} \quad (23)$$

$$\begin{aligned} F(\rho^{(1)}, \rho'^{(1)}) &= \sum_{k \in \mathcal{B}} \frac{\text{Tr}(e^{-C_k/2})}{\sqrt{\text{Tr}(e^{-\beta H_k}) \text{Tr}(e^{-\beta' H'_k})}} \\ &= \sum_{k \in \mathcal{B}} \frac{\sqrt{2(1 + \cosh(E_k/2T) \cosh(E'_k/2T') + \sinh(E_k/2T) \sinh(E'_k/2T') \vec{n}_k \cdot \vec{n}'_k)}}{\sqrt{2 \cosh(E_k/2T) 2 \cosh(E'_k/2T')}} \end{aligned} \quad (24)$$

Many-Body

$$\begin{aligned} F(\varrho^{(0)}, \varrho'^{(0)}) &= \prod_{k \in \mathcal{B}} \frac{\text{Tr}(e^{-C_k/2})}{\text{Tr}(e^{-\beta \mathcal{H}_k}) \text{Tr}(e^{-\beta' \mathcal{H}'_k})} \\ &= \prod_{k \in \mathcal{B}} \frac{\det(I + e^{-C_k/2})}{\det^{1/2}(I + e^{-\beta H_k}) \det^{1/2}(I + e^{-\beta' H'_k})} \\ &= \prod_{k \in \mathcal{B}} \frac{2 + \sqrt{2(1 + \cosh(E_k/2T) \cosh(E'_k/2T') + \sinh(E_k/2T) \sinh(E'_k/2T') \vec{n}_k \cdot \vec{n}'_k)}}{\sqrt{[2 + 2 \cosh(E_k/2T)][2 + 2 \cosh(E'_k/2T')]} \end{aligned} \quad (25)$$

$$\begin{aligned} F(\varrho^{(1)}, \varrho'^{(1)}) &= \prod_{k \in \mathcal{B}} \frac{\text{Tr}(e^{-(C_k - \log(Z_k)n_k - \log(Z'_k)n'_k)/2})}{\text{Tr}(e^{-(\beta \mathcal{H}_k - \log(Z_k)n_k)}) \text{Tr}(e^{-(\beta' \mathcal{H}'_k - \log(Z'_k)n'_k)})} \\ &= \prod_{k \in \mathcal{B}} \frac{\det(I + e^{-C_k/2 - \log(Z_k)/2 - \log(Z'_k)/2})}{\det^{1/2}(I + e^{-(\beta H_k - \log(Z_k))}) \det^{1/2}(I + e^{-(\beta' H'_k - \log(Z'_k))})} \\ &= \prod_{k \in \mathcal{B}} \left(1 + \frac{[2(1 + \cosh(E_k/2T) \cosh(E'_k/2T') + \sinh(E_k/2T) \sinh(E'_k/2T') \vec{n}_k \cdot \vec{n}'_k)]}{\sqrt{(2 \cosh(E_k/2T))(2 \cosh(E'_k/2T'))}} \right. \\ &\quad \left. + \frac{1}{(2 \cosh(E_k/2T))(2 \cosh(E'_k/2T'))} \right) \times \left(\sqrt{[2 + (2 \cosh(E_k/2T))^{-2}][2 + (2 \cosh(E'_k/2T'))^{-2}]} \right)^{-1}, \end{aligned} \quad (26)$$

where the single-particle partition function for momentum k , Z_k , is given by

$$Z_k = \text{Tre}^{-H_k/T} = 2 \cosh(E_k/2T), \quad (27)$$

the matrix C_k is such that $e^{-C_k} = e^{-\beta H_k/2} e^{-\beta' H'_k} e^{-\beta H_k/2}$ and $C_k = \Psi_k^\dagger C_k \Psi_k$ is the corresponding many-body quadratic operator.